Biomaterials 35 (2014) 6323–6331

Contents lists available at ScienceDirect

Biomaterials

journal homepage: www.elsevier.com/locate/biomaterials

Nanoparticle toxicity assessment using an *in vitro* 3-D kidney organoid culture model

Anna I. Astashkina [a,1], Clint F. Jones [a,1], Giridhar Thiagarajan [b], Kristen Kurtzeborn [b], Hamid Ghandehari [a,b,c], Benjamin D. Brooks [a], David W. Grainger [a,b,c,*]

[a] Department of Pharmaceutics and Pharmaceutical Chemistry, University of Utah, Salt Lake City, UT 84112-5820, USA
[b] Department of Bioengineering, University of Utah, Salt Lake City, UT 84112-5820, USA
[c] Utah Center for Nanomedicine, Nano Institute of Utah, University of Utah, Salt Lake City, UT 84112-5820, USA

ARTICLE INFO

Article history:
Received 26 February 2014
Accepted 16 April 2014
Available online 10 May 2014

Keywords:
Nephrotoxicity
3-D cell culture
Gold nanoparticles
PAMAM dendrimers
Proximal tubules
In vitro–in vivo correlations

ABSTRACT

Nanocarriers and nanoparticles remain an intense pharmaceutical and medical imaging technology interest. Their entry into clinical use is hampered by the lack of reliable *in vitro* models that accurately predict *in vivo* toxicity. This study evaluates a 3-D kidney organoid proximal tubule culture to assess *in vitro* toxicity of the hydroxylated generation-5 PAMAM dendrimer (G5-OH) compared to previously published preclinical *in vivo* rodent nephrotoxicity data. 3-D kidney proximal tubule cultures were created using isolated murine proximal tubule fractions suspended in a biomedical grade hyaluronic acid-based hydrogel. Toxicity in these cultures to neutral G5-OH dendrimer nanoparticles and gold nanoparticles *in vitro* was assessed using clinical biomarker generation. Neutral PAMAM nanoparticle dendrimers elicit *in vivo*-relevant kidney biomarkers and cell viability in a 3-D kidney organoid culture that closely reflect toxicity markers reported *in vivo* in rodent nephrotoxicity models exposed to this same nanoparticle.

1. Introduction

Nanoparticle-based drug delivery systems, imaging agents, and diagnostic products are commonly advocated for their perceived substantial new biomedical applications and improved performance [1]. The nanotechnology-based medical market is predicted to amount to $1 trillion dollars [2] and to involve up to half of all pharmaceutical products by 2015 [3]. This rapid expansion of nano-sized biomedical technologies for human use is greatly limited by poor understanding of how these materials' unique physico–chemical and dimensional characteristics influence biological systems, particularly toxicity mechanisms [4]. Nanotoxicology studies seek to develop assays to address the unique challenges of cellular uptake, distribution, accumulation, immune system activation, and protein milieu interactions associated with nano-sized materials [5,6]. Currently, cell-based assays are the standard method of cell-nanomaterial assessment despite consistent lack of *in vitro–in vivo* correlations or *in vitro* data reliability and reproducibility [5]. Many reviews addressing this topic consistently emphasize the compelling need for more clinically relevant *in vitro* assay systems to facilitate both basic studies of nanomaterial interactions with physiological systems that reliably elucidate specific injury mechanisms, as well as translational research predictive of nano-sized materials toxicity [5–12].

Nephrotoxicity is a central feature in many adverse drug responses due to the kidney's central roles in metabolism and blood filtration that combine to produce high toxic metabolite concentrations in the kidney proximal tubules [13]. With increasing use of nanoparticle carriers in drug formulation, the toxicity profiles of such carriers must also be well defined. Nanoparticle studies *in vivo* consistently show access and biodistribution to the kidney once systemically bioavailable [14]. The unique size and concentration aspects of the kidney environment make nephrotoxicity an important consideration for both drug/metabolite and nanocarrier safety evaluations. Several studies describing nanoparticle toxicity *in vivo* found that opsonization, size, structure and dose are key factors that influence induction of toxicity [15]. Specifically, anionic particles [16] in colloidal suspensions (size greater than 13 nm) [17] tend to be less toxic and have lower immunoglobulin (IgG) binding [18]. However, specifically for gold, nanoparticles as small as 5 nm

* Corresponding author. Department of Pharmaceutics and Pharmaceutical Chemistry, University of Utah, Salt Lake City, UT 84112-5820, USA. Tel.: +1 801 581 3715; fax: +1 801 581 3674.
E-mail address: david.grainger@utah.edu (D.W. Grainger).
[1] These authors contributed equally to this work.

http://dx.doi.org/10.1016/j.biomaterials.2014.04.060
0142-9612/

produced few detectable transcriptional changes when exposed to primary human umbilical vein endothelial (HUVEC) cells *in vitro* [19] but attenuated collagen-induced arthritis in a mouse model through inhibition of angiogenesis [20,21], and showed possible toxicity in liver and spleen as 1.5-nm gold nanoparticles [22]. These and other reports of gold's *in vitro–in vivo* problematic toxicity correlations are inconsistent across gold preparations and particle size scales [11]. As many studies evidence gold nanoparticle distribution to the kidney [14] [22], *in vitro* toxicity models that screen and predict this reliably and provide *in vitro–in vivo* validation would be a substantial advantage. Lastly, with regard to PAMAM dendrimers, previous *in vivo* studies using G5-OH PAMAM dendrimers [23] reported kidney accumulation without significant up-regulation of kidney injury biomarkers – creatinine and blood urea nitrogen (BUN) [24]. However, the lack of validated standardized protocols, verified *in vitro* nanocarrier-suitable assays for nephrotoxicity and endotoxin-free procedures all hamper reliable toxicity determinations [15].

Recently, a three-dimensional (3-D) organoid kidney proximal tubule epithelial cell culture (Fig. 1A) was described for assessment of drug toxicity *in vitro* [25,26]. Unlike other cell-based culture systems reported for drug screening, this model utilizes unique culture conditions that preserve primary cells for weeks *in vitro* without significant changes in kidney cell phenotype. Furthermore, the tissue replacement kidney model was shown to respond to environmental agents with clinically relevant toxicity indicators previously described only in preclinical animal drug toxicity studies. These markers included induction of kidney injury molecule 1 (Kim-1) and nephrotoxicity-associated genes, shedding of cell-associated enzymes N-acetyl-ß-D-glucosaminidase (NAG) and ɣ-glutamyl transferase (GGT), and release of inflammatory proteins. The 3-D kidney model has been extensively validated for 2 months of proximal tubule phenotype stability and cell functionality [26]. Furthermore, it has been a subject of 2-D to 3-D comparisons using a variety of environmental toxins [25].

In this study, this 3-D organoid kidney proximal tubule cell culture model is extended to analyze its ability to replicate *in vivo* toxicity imposed by gold nanoparticles and G5-OH PAMAM dendrimers. Both gold nanoparticles and dendrimers analyzed were less than 6 nm in size to ensure kidney clearance [27] *in vivo* independent of particle charge [28]. Since most common toxicity modes associated with nano-sized particles involve inflammation, DNA damage and cellular damage [29,30], assays were chosen that reflected these pathways. In order to further characterize possible nanotoxicity for these nanoparticles and also to assess the value of this 3-D tissue culture model for nanoparticles, the *in vitro* nephrotoxicity of both G5-OH PAMAM dendrimers and gold nanoparticles was assessed using DNA- and cell membrane integrity-assessing cell viability studies, immunohistochemistry for putative biomarkers and inflammatory cytokine assays.

2. Materials and methods

Murine kidney organoid proximal tubule 3-D cell cultures were prepared as described previously [25,26]. All procedures involving rodents were approved by the University of Utah Institutional Animal Care and Use Committee. Briefly, freshly sacrificed mouse kidneys from male *C57BL/6* mice (Jackson Laboratories, USA) were surgically aseptically removed and cleaned. Kidneys were mechanically and enzymatically digested and then filtered to isolate the proximal tubules (PT). PTs were resuspended in biomedical grade hyaluronic acid (HA) hydrogel (SentrX Animal Care, USA) to yield approximately 5000 PTs/50 μL of gel. HA gels were fabricated using 1.5% thiol-modified carboxymethylated HA (CMHA-S) and 7.5% poly(ethylene glycol) diacrylate (PEGDA) bifunctional electrophile crosslinker in sterile Phosphate Buffered Solution (PBS++, (Invitrogen, USA)) aqueous media. 3-D HA gel constructs containing suspended PTs in PBS were then cast into TeflonAF®-coated 96-well plates [31] and allowed to crosslink via spontaneous Michael addition chemistry in the presence of suspended viable PTs for 35 min in a cell incubator at 37°C. These gelled PT organoid constructs were incubated in phenol red-free proximal tubule media (PT media) consisting of 1% fetal calf serum (Invitrogen, USA), 5% sodium pyruvate (Invitrogen, USA), 1% non-essential amino acids (Invitrogen, USA), 1% insulin/transferrin/selenium (Invitrogen, USA), 1% antibiotic-antimycotic (Invitrogen, USA), 0.9 μg of hydrocortisone (Invitrogen, USA) and DMEM-Ham's F-12 with HEPES and L-glutamine (Invitrogen, USA). Cell media was manually exchanged every 2 days for maximum viability. All 3-D gels were utilized for toxicity experiments 2 days after their preparation. These conditions have been shown to produce viable kidney PT toxicity biomarkers for 6–8 weeks [25,26].

Nanoparticles were prepared using common preparation protocols. Gold nanoparticles were prepared by chloroauric acid (0.01%) reduction as previously described [32,33]. Gold nanoparticles were sized by measuring 120 particles on a TEM micrograph (University of Utah Imaging Core Facility, USA) using ImageJ software. As reported previously [34], G5-COOH PAMAM dendrimers (Sigma Aldrich, USA) were purified using preparative size exclusion chromatography (SEC, Sephadex Hiload 75, GE Healthcare, Piscataway, USA) and labeled with fluorescein isothiocyanate (FITC) [34,35]. Residual FITC was then removed by dialysis in deionized water (500 Da molecular weight cutoff membranes, Spectrum Laboratories, USA) and then by preparative size exclusion chromatography (*vide supra*). The absence of small molecular weight impurities was assessed by analytical size exclusion chromatography (Superose 6 10/300 GL, GE Healthcare, Piscataway, USA). This method has been previously shown to produce ~1.3 fluorescein labels per dendrimer (mol/mol) [34].

Toxicity of these nanomaterials in the 3-D PT culture system was assessed using nanoparticle concentrations approximating those that kidney proximal tubule epithelial cells might realistically experience *in vivo*: G5-OH PAMAM dendrimer concentrations at 0.675 mg/mL (high dose) and 0.05 mg/mL (low dose) (i.e., the ranges of intravenous dendrimer exposure previously used in an *in vivo* rodent nephrotoxicity study) [24], and gold nanoparticles at 56.6 μg/mL (high dose) and 3.5 μg/mL (low dose) [36]. The doses were calculated assuming nanoparticles were partitioned in the blood compartment after injection. The 3-D kidney organoid cultures were incubated with both high (0.675 mg/mL) and low (0.05 mg/mL) doses of G5-OH PAMAM dendrimers or 56.6 μg/mL of gold nanoparticles separately for 48 h, and known nephrotoxin, cisplatin [22,23] (1.7 mM, positive control, Sigma

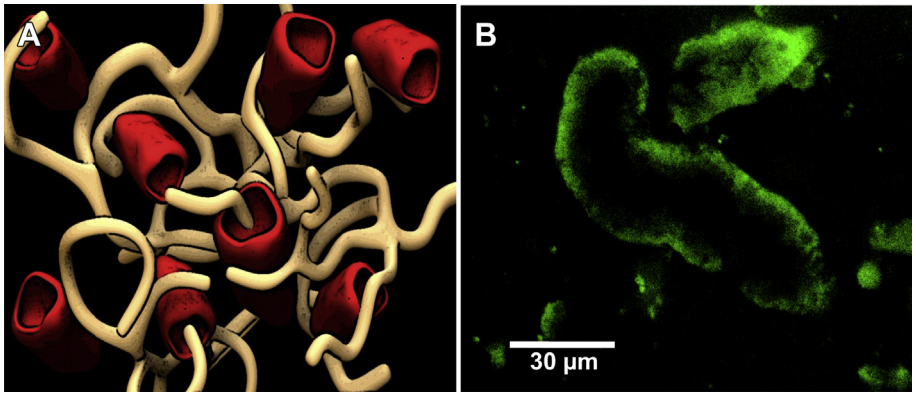

Fig. 1. A) Conceptual graphic depicting 3-D organoid culture design with kidney PTs (red) surrounded by HA hydrogel encapsulating matrix (tan fibrils); B) fluorescent micrograph of actual 3-D PT *in vitro* culture after 30 min exposure to fluorescein-labeled G5-OH dendrimer in PT media (For interpretation of the references to colour in this figure legend, the reader is referred to the web version of this article).

Aldrich, USA), for 72 h (final concentrations). *Cisplatin was prepared for each experiment by diluting a 200 mM stock solution in dimethyl sulfoxide (DMSO) into PT media and sterile filtering (0.22 μm cell culture filter) the solution. Gold nanoparticles and dendrimers were applied to the top ambient exposed surface of the gel cultures as homogeneous suspensions in PT media.* PT epithelial cell viability was assessed after 48 h of incubation with gold nanoparticles or dendrimer. All PT viability experiments used two technical replicates (mice) and three independent measurements (redundant PT cultures).

To more closely parallel kidney exposure in a previous G5-OH dendrimer *in vivo* rodent toxicity study [24] and assess the utility of this *in vitro* PT organoid culture model to confirm *in vivo* kidney nanotoxicology results, *C57BL/6* mice were injected with G5-OH PAMAM dendrimers in sterile 150 mM NaCl as described previously [24]. G5-OH PAMAM dendrimers in 150 mM NaCl and vehicle-only controls were assigned to three-animal cohorts. Each mouse received a single i.v. tail vein injection (100 μL) of 0.675 mg/mL dendrimer in this vehicle. At the previously established time of peak kidney dendrimer accumulation (i.e., 2 h post-injection) [24], mice were euthanized to permit harvest of kidney PTs freshly pre-exposed to systemic dendrimer dosing mimicking the previous *in vivo* study [21]. These PTs were harvested immediately and prepared as described above into the 3-D PT constructs in HA culture media. These cultures were maintained for 22 days and cell viability was assessed every 3 days.

In all 3-D PT cultures, cell-associated kidney injury molecule-1 (Kim-1) and tumor necrosis factor (TNFα) were assessed as previously described [25,26]. PT cell viability studies were performed using CyQuantNF® fluorescent assay (Invitrogen, USA). All solutions were made according to manufacturer's instructions. CyQuantNF® was applied directly to 3-D organoid cultures and incubated for 1 h in the cell culture incubator. Media above the gel constructs was collected and analyzed using a microplate reader (Synergy 2, Biotek, USA) using *fluorescence (*485 nm excitation and 530 nm emission filters). Collected cell numbers were normalized to untreated controls as percent survival. Immunohistochemistry was performed for *in vivo* biomarkers of kidney toxicity, Kim-1 and TNFα. At the end of nanoparticle exposure incubations, 3-D organoid cultured were washed 2× with PBS, fixed using 4% paraformaldehyde overnight at 4 °C, incubated with Image-iT® FX signal enhancer (Molecular Probes, USA), and stained using 1:500 dilution of Kim-1 R9 primary antibody or 1:1000 dilution of TNFα-PE antibody (eBiosciences, USA). After incubation, excess Kim-1 stain was washed away using PBS and exposed to secondary Alexa-488 anti-rabbit antibody (Invitrogen, USA). All constructs were imaged at 400× using Olympus FV1000 Spectral confocal microscope (University of Utah Core Imaging Facilities, USA).

In addition to cell viability, other general health kidney biomarkers were evaluated. Shedding of NAG is a sign of proximal epithelial cell necrosis [37]. NAG shedding was evaluated using previously published protocols [38]. Briefly, NAG appearance in the media of the 3-D organoid cultured was measured after 48-h nanoparticle incubations after which 100 μL of media was removed and incubated with 100 μL of 2.24 mM *p*-nitrophenyl-*N*-acetyl-*β*-D-glucosaminide (Sigma Aldrich, USA) in citrate/phosphate solution (0.1 M citric acid, 0.1 M Na_2HPO_4, pH 4.5). The amount of NAG lysosomal enzyme was assessed by measuring 4-nitrophenol product formation against known 1 mM 4-nitrophenol standard (Sigma Aldrich, USA). Increases in optical absorbance in treated 3-D PT cultures over untreated cultures were measured at 405 nm. Lastly, expression of inflammatory cytokines by PT cells was measured using a MILLIPLEX MAP Mouse Cytokine/Chemokine Premixed 22-Plex mouse cytokine kit (Millipore, USA). Concentrations of IL-1β, IL-2, IL-6, IL-10, TNFα, INFγ, MCP-1, MIP-1α, MIP-1β, MIP-2, and RANTES were assessed according to manufacturer's instructions. Standard curves were run for each cytokine in PT media to determine the dynamic range of the assay. Cytokines in the media were measured using the Luminex Magpix system. A minimum of 30 bead counts were accepted for each cytokine assay. Measured cytokine concentrations were adjusted according to cell viability data to represent the amount of soluble protein detected/5000 PTs.

Transport and availability of added nanoparticles to PT cultures within the HA-based encapsulation gel were assessed by simple optical evaluations of nanoparticle transport through empty HA gels (i.e., no cells or PTs encapsulated). Gels were fabricated by loading the identical HA polymer liquid mixture within Transwell® inserts in PT media (as described above for 96-well culture plates) and allowed to cure for 30 min and then placed in wells containing PT liquid culture media. Gold nanoparticle suspensions or dendrimer solutions were added to the top (i.e., ambient exposed) side of the gel-coated Transwell® insert and particle diffusion through the gel was noted qualitatively as a color change in the receiver fluid beneath the Transwell® insert. Separately, gold nanoparticles and dendrimers were both observed to diffuse freely through the Transwell® membrane lacking HA gel (visual observation, data not shown). As a secondary assessment of gold nanoparticle gel transport, HA gels were synthesized by loading the HA polymer liquid mixture inside a rubber o-ring sandwiched between two layers of filter paper. This assembly was then clamped between the two halves of a glass Franz diffusion cell. After HA gel curing, PT media was loaded in the receiver side of the Franz cell assembly and gold nanoparticles (56.6 μg/mL) were loaded into the donor side in PT media. Aliquots were collected from the receiver cell at various time points (at ambient temperature) and particle diffusion was determined by sample optical absorbance at the gold nanoparticle plasmon peak (520 nm, Biotek Synergy II plate reader).

3. Statistics

All data analysis used Excel 2010 (Microsoft, USA) and GraphPad Prism 5 (GraphPad Software, Inc., USA). All cell experiments were performed using three to seven independent samples with two technical replicas. All independent samples used cells isolated from different mice. Data were compared and evaluated pairwise using ANOVA. Observations were considered to be statistically significant with $p < 0.05$.

4. Results

In vitro 3-D kidney organoid PT viability changes and toxicity markers were assessed using nanoparticle dose–response curves for PT cytokine expression, Kim-1, and induction of NAG shedding into the 3-D culture media. Dose–response curves for G5-OH PAMAM dendrimers were assessed over ranges of intravenous dendrimer exposure previously used in an *in vivo* rodent study [24].

Both G5-OH dendrimers and gold nanoparticles were characterized as reported previously in cell penetration studies [39]. G5-OH dendrimers exhibited an average hydrodynamic radius of 2.6 ± 0.17 nm as measured by dynamic light scattering (DAWN HELEOS II, Santa Clara, USA) and a zeta potential of 0.015 ± 6.8 mV in deionized water (pH adjusted to 7.4, not buffered) as measured by Zetasizer Nano ZS (Malvern, Westborough, USA). Gold nanoparticles exhibited an average size of 5.2 ± 1.3 nm and variable negative zeta potential in chloride-containing media.

Nanoparticle transport studies showed drastically different results for the G5-OH dendrimers and gold nanoparticles in the HA gel culture matrix (Fig. 2). Transwell®-supported gel diffusion studies for G5-OH-FITC transport indicated facile dendrimer diffusion through these HA gels in less than 10 min (visual observation, data not shown). However, Transwell® and Franz cell transport experiments for the gold nanoparticles both indicate major transport problems in the HA matrix. Gold nanoparticles failed to effectively diffuse through the HA hydrogel, binding instead to the HA gel (data not shown), thus compromising their distribution throughout the PT cultures. This matrix-binding compromised the validity of the culture-based gold nanomaterial toxicity results. Mechanisms of HA gel entrapment could involve calcium ion bridging between negatively charged gold nanoparticles and the carboxylated HA matrix, or more complex binding phenomena involving adsorbed protein coronas on the gold surface. Both steric issues with physical immobilization and particle sieving within the crosslinked HA gel could be involved. Hence, initial PT culture toxicity results using 56.6 μg/mL (high dose) and 3.5 μg/mL (low dose) gold nanoparticle exposures in PT media, showing minimal observed toxicity markers, were considered artifactual (data not shown). No further gold nanoparticle toxicity assessments were therefore performed or reported here for these PT culture systems.

PT cell viability after 48 h of G5-OH dendrimer exposure evidenced limited cell toxicity. At the highest concentrations used (0.8 mg/mL), G5-OH PAMAM dendrimers produced ~20% cell death, comparable to non-treated control PT cell cultures (comparison in Fig. 2A). These measurements were confirmed by shed NAG concentration assessments in PT media. NAG is a lysosomal enzyme commonly measured *in vivo* as a signature of proximal tubule damage [37]. These finding were supported at high and low ends of the G5-OH PAMAM dose–response curves, corresponding to 0.675 mg/mL and 0.05 mg/mL dendrimers, respectively. No statistically significant NAG up-regulation at any of the tested concentrations compared to untreated controls was observed (Fig. 2B) unlike previously observed in this 3-D culture [25]. Cumulatively, these data suggest that G5-OH PAMAM dendrimers do not cause

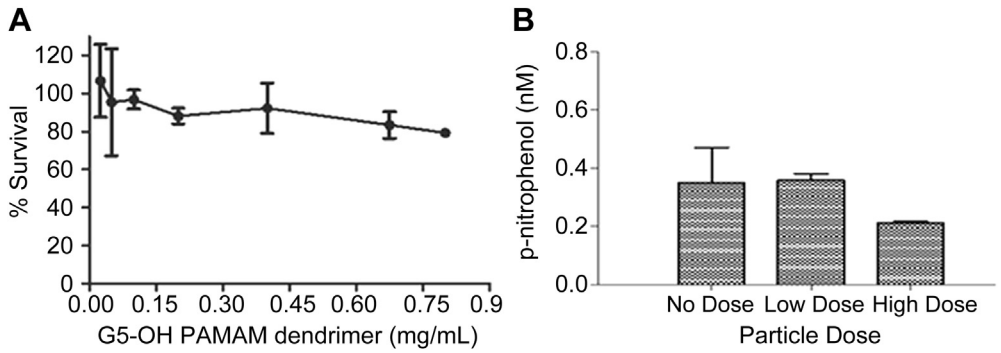

Fig. 2. PT cell viability results from 3-D organoid cultures 48 h after G5-OH PAMAM dendrimer exposure using A) CyQuant NF DNA-binding assay over a broad range of G5-OH doses, and B) NAG release into the culture media at 0.675 mg/mL (high dose) and 0.05 mg/mL (low dose) i.e., the range of intravenous dendrimer exposure previously used in an *in vivo* rodent nephrotoxicity study [21] ($n = 3$, 2 technical replicas).

significant cell toxicity in the 3-D organoid proximal tubule cell culture at this dosing range at single-dose 48-h exposures.

In addition to NAG, up-regulation of both Kim-1 and TNFα markers *in vivo* are commonly associated with PT epithelial cell damage [40,41]. Nephrotoxic drugs, such as cisplatin [25,26], are shown to correlate with both kidney toxicity and NAG shedding, and also the up-regulation of both Kim-1 and TNFα. Protein induction in response to G5-OH PAMAM dendrimers was measured after 48 h of dendrimer exposure and compared to no-treatment 3-D proximal tubule culture (negative control) and also the nephrotoxic drug cisplatin (1.7 mM, positive control) previously shown to up-regulate Kim-1 and TNFα in animal models and in the 3-D tissue PT culture system [25,26]. The high concentration (0.675 mg/mL) G5-OH PAMAM dendrimer dosing was used. As shown in Fig. 3, both Kim-1 and TNFα were significantly induced in response to this G5-OH PAMAM dendrimer dose compared to negative control (vehicle-only). No apparent difference in TNFα up-regulation between cisplatin positive control and the dendrimer was observed; in contrast, Kim-1 induction was lower for G5-OH PAMAM dendrimers compared to cisplatin-treated PT epithelial cell cultures (Fig. 3). These data show that the G5-OH dendrimer induces some PT cellular damage also reflected in expression of known inflammatory cell markers of toxicity (vida infra), but not to the extent associated with potent clinical nephrotoxic agents [41].

Production of soluble cytokines by PT epithelial cells was measured using the Luminex bead assay system that collects and averages data from a minimum of 30 beads per measurement. The dynamic range of these assays was asserted using PT media cytokine-spiked 6-point standard curves. The typical assay ranges found were: 35.99 pg/mL to 1940.86 pg/mL for IL-1β; 1.02 pg/mL to 2073.45 pg/mL for IL-2; 0.85 pg/mL to 2128.89 pg/mL for IL-6; 1.76 pg/mL to 1844.77 pg/mL for IL-10; 1.07 pg/mL to 1909.63 pg/mL for TNFα; 1.14 pg/mL to 2669.15 pg/mL for INFγ; 6.41 pg/mL to 1976.37 pg/mL for MCP-1; 11.16 pg/mL to 3758.46 pg/mL for MIP-1α; 1.84 pg/mL to 1871.94 pg/mL for MIP-1β; 91.28 pg/mL to 4168.24 pg/mL for MIP-2; 0.93 pg/mL to 1986.38 pg/mL for RANTES. Expression of IL-1β, IL-2, IL-6, IL-10, TNFα, INFγ, MCP-1, MIP-1α, MIP-1β, MIP-2, and RANTES proteins was assessed after PT organoid 48-h culture incubations with high (0.675 mg/mL) G5-OH PAMAM dendrimer concentrations (Fig. 4 and Supplemental Fig. 1). Results indicate that most cytokines produced by PT exposure to G5-OH dendrimers were comparable to negative controls and also statistically different than the cisplatin positive control cytokine expression.

Data shown in Fig. 5 attempt to provide a direct comparison of PT toxicity development from G5-OH dendrimer nanoparticle exposures in PT 3-D cell culture to that reported for the same exposure to kidney *in vivo*. Specifically, G5-OH murine kidney

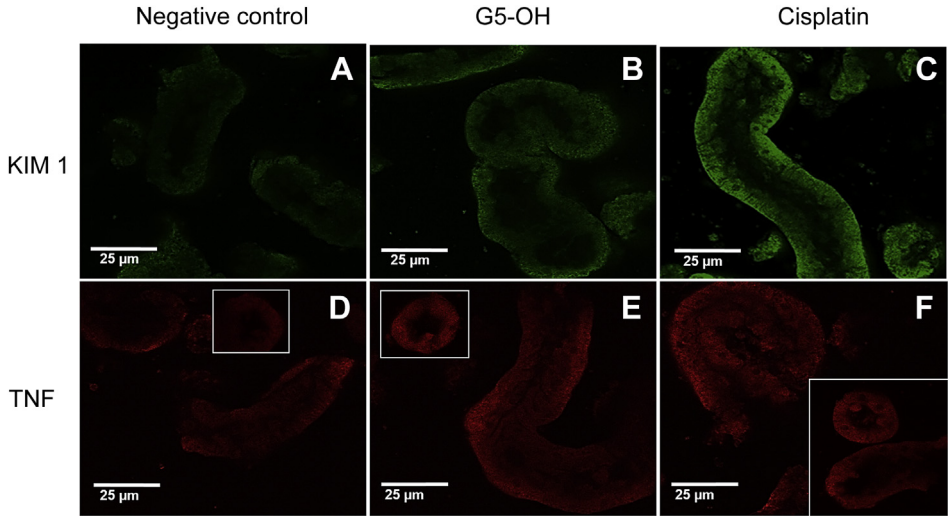

Fig. 3. Immunohistochemistry fluorescent microscopy observations of kidney PT biomarkers KIM1 and TNF-alpha as indicators of PT damage after 48 h of agent incubation: A) and D) no treatment; B) and E) after exposure to the high dose (0.675 mg/mL) of G5-OH PAMAM dendrimer; C) and F) after treatment with cisplatin (1.7 mM positive control nephrotoxin).

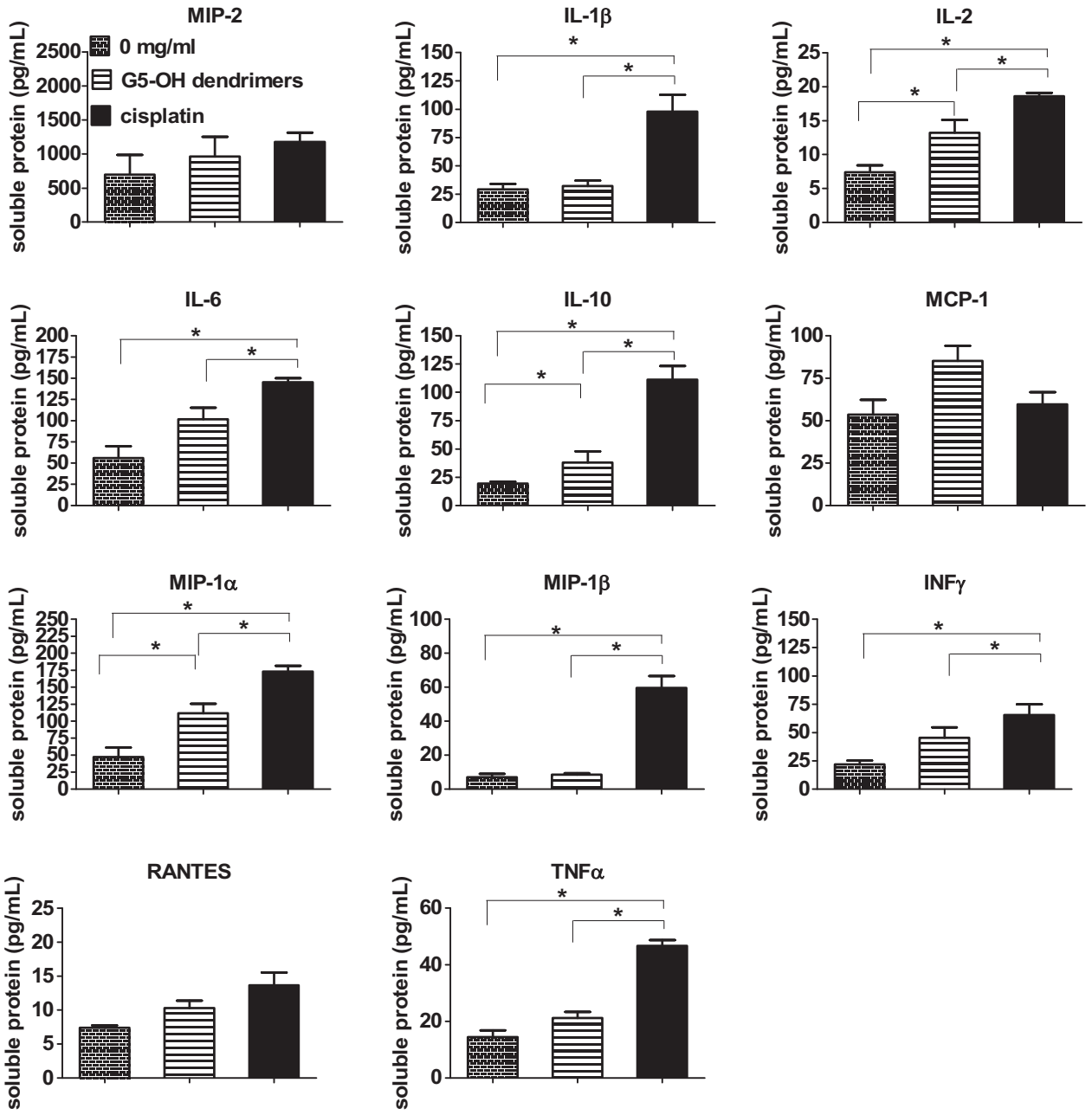

Fig. 4. Cell cytokine expression profiles from PT epithelial cells after 48 h of incubation with G5-OH PAMAM dendrimers (high concentration (0.675 mg/mL) dosing) compared to empty vehicle (negative control) and known nephrotoxin cisplatin (positive control, 1.7 mM) in 3-D PT organoid cultures ($n = 3–7$, mean ± SEM).

accumulations *in vivo* from tail vein injections were compared using direct kidney harvest, PT isolation and extended PT culture in the HA 3-D constructs *in vitro*. The model showed that, similar to previous mouse toxicity assessment using traditional clinical biomarkers, BUN and creatinine [24] little influence on culture PT epithelial cell viability could be associated with *in vivo* renal exposure to the PAMAM dendrimer compared to vehicle-only injection controls (Fig. 5).

5. Discussion

Current innovations and improvements in 3-D tissue replacement systems in terms of availability and diversity of materials, support structures and understanding of relationships between cell culture complexity and *in vivo*-relevant data acquisition have contributed immensely to facilitate and embrace the substantial preclinical potential of these *in vitro* models. Previously, we have described a 3-D culture model of kidney toxicity that used isolated proximal epithelial tubules sustained in chemically modified HA matrix [25,26]. The strength of the model was in retaining the primary tissue associated with drug toxicity, proximal epithelial cells, within their native environment that included cell–cell and cell-ECM interactions. The model was shown to sustain its cell differentiation potential and functionality for up to 6 weeks in a static culture [26].

Kidney proximal tubule endothelial cell phenotypic functionality was evaluated as a series of bi-weekly enzymatic activity assays that tested their capability to process proteins from the media (cathepsin B), maintain ligands for biotransformation (γ-glutamyltransferase) and endocytosis (megalin), and continue signaling

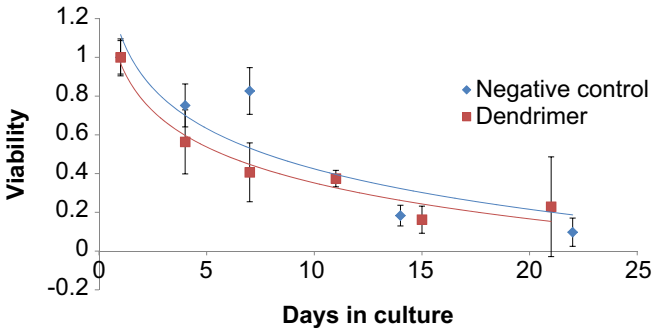

Fig. 5. Normalized kidney PT cell viability in 3-D *in vitro* organoid cultures derived from murine kidneys after tail vein injection of G5-OH PAMAM dendrimers or empty vehicle (negative control) into mice with harvest of kidneys 2 h post-injection ($n = 3$, 2 technical replicas).

molecule dephosphorylation (alkaline phosphatase (AP)). Similarly, cell phenotypic identity retention was assessed through evaluation of molecular markers for proximal tubule-specific aquaporin (AQP1), megalin ligand, cytochrome P450 enzymes and *Phaseolus vulgaris* erythroagglutinin (PHA-E) staining at 2 months. The cells appeared to sustain their native environment interactions for the entire 2 months of evaluation, as perceived by confocal microscopy and evaluation of gap junctions (Connexin 43), integrins (α_3) and cell polarization (organic anion transporter 1 (OAT 1)) transporter localization [26]. Moreover, when tested for drug toxicity side by side with immortalized cell lines, LLC-Pk1 and HEK293, it was proven to have a wide range of toxicity biomarkers that previously were only found to be induced in animal models [25]. Specifically, the 3-D culture responded to toxic drugs with up-regulation of Kim-1 and nephrotoxicity-associated genes, neutrophil gelatinase-associated lipocalin (NGAL), osteopontin (Spp1), clusterin (CLU), vimentin (VIM), heme oxygenase-1 (HO-1) shedding of cell-associated enzymes N-acetyl-ß-D-glucosaminidase (NAG) and ɣ-glutamyl transferase (GGT); release of inflammatory proteins, TNFα, MCP-1, IL-6, IL-1β, MIP-1α, and RANTES proteins; and *in vivo*-relevant down-regulation of CYP2E1 enzymes. This extensive 2-D to 3-D evaluation of the model showed significant differences between traditional methods of kidney toxicity evaluation and 3-D culture [25]. Unlike 3-D model, transformed cell lines had limited number of biomarkers that could even be measured and proved to provide a poor correlation to *in vivo* literature-supplied data.

In this work we extend our previous findings of 2-D to 3-D comparisons to evaluating 3-D culture to *in vivo*-acquired data. Specifically, *in vitro* 3-D primary kidney organoid PT epithelial cell cultures were exposed to gold nanoparticles and G5-OH-terminated PAMAM dendrimers since both nanoparticles have comparative biodistribution and nephrotoxicity data published from *in vivo* rodent models for direct comparison. The *3-D PT organoid culture* approach represents a new nephrotoxicity diagnostic tool and screening method for drugs [25,26] and for some nanoparticles where their transport is appropriately unhindered in this anionic hydrogel matrix.

The strategy offers an important transition model between 2-D *in vitro* cell monolayers on rigid plastic [30], often irrelevant and tedious, and the more expensive *in vivo* preclinical animal models. The 3-D kidney PT organoid model was previously validated using known soluble small molecule nephrotoxic agents [25,26] with a variety of injury initiation markers. Unlike primary or immortalized cells cultured using traditional approaches that respond to bioactive agents with limited *in vivo*-relevant indicators, the 3-D HA gel constructs exhibited induction of a wide range of commonly used *in vivo* biomarkers, such as PT surface protein Kim-1, shedding of NAG and GGT enzymes, release of TNFα, MCP-1, IL-6, IL-1β, MIP-1α, and RANTES cytokines, down-regulation of CYP2E1 metabolic enzyme, and induction of NGAL, VIM, CLU, HO-1, Spp1 nephrotoxicity-associated genes [25,26]. All these biomarkers are considered to be putative markers of PT epithelial cellular damage in human and animal models through either induction of inflammation, defense mechanisms or damage of cell wall integrity [37,40–44].

Reported success of the PT culture model was attributed to preservation of the contextual communication characteristics of the *in vivo* kidney tissue microenvironment, which for kidney toxicity was associated with maintenance of the intact, viable PTs *in vitro* [26]. Furthermore, a significant advantage of the 3-D model proved to be the long-term sustainability of the primary differentiated PT epithelial phenotype in culture, which extends opportunities for testing kidney toxicity not only in terms of acute but also accumulated kidney cellular damage. The current work exploits this advantage to evaluate the model for nanoparticle toxicity in 3-D PT organoid culture with direct comparison to nephrotoxicity biomarkers produced in the corresponding mouse *in vivo* kidney toxicity model. Results show that the (3-D) organoid culture system serves consistently in that capacity, mirroring results found *in vivo* for the G5-OH PAMAM dendrimer. However, like all cellular and *in vivo* animal models, 3-D culture is not a foolproof method and understanding its limitations is critical for its successful implementation. Specifically, it is important to appreciate that brining in additional complexity adds new variables that need to be addressed in assay development. Natural and synthetic polymers and biomaterials commonly used to support cell and organoid growth in 3-D have their own physiochemical characteristics and are bound to affect diffusion characteristics, time exposures and choice of assays due to matrix-assay interactions. For example, majority of the popular choices for 3-D matrices such as Matrigel®, extracellular matrix (ECM), collagen, fibrinogen, alginate, chitosan, dextran, polyacrylamide and HA hydrogels have a native charge distribution that can adsorb and limit diffusion of charged drugs, nanoparticles, nucleic acids, proteins and other charged molecular species commonly assessed in cell-based assays. Hence, it is critical to assess 3-D matrix-assay and matrix-nanoparticle/drug interactions beyond the cellular biocompatibility.

In this paper we present two type of nanoparticles with compatible sizes that proved to have different diffusion characteristics throughout the HA gel. Gold nanoparticles exhibited significant binding to the HA gel matrix, hindering their transport and uniform distribution within the culture medium upon dose introduction. Both Franz cell and Transwell®-based gold nanoparticle transport experiments showed the consistent inability of these gold nanoparticles to freely diffuse through the 3-D organoid PT cell culture matrix to gain uniform access to the PT cells under dosing.

Two explanations are offered to account for this gold-matrix binding. First, these commercial HA 3-D hydrogel biomaterials are deliberately thiolated in order to crosslink spontaneously through Michael addition chemistry [45,46]. Unreacted, exposed thiol groups on HA could react with gold surfaces to form stable gold-thiolate bonds, hindering particle diffusion through the HA gel. This is supported by the disappearance of the characteristic red plasmonic color of the gold nanoparticle solutions and resulting formation of a dark layer deposited onto the proximal edge of the HA gel where the gold nanoparticles were loaded, supporting particle aggregation. Importantly, since large classes of nanoparticles including gold, silver, copper, quantum dots, and some derivatized silicas react with thiol chemistry, identifying and overcoming this problem is critical to future extensions of this 3-D matrix approach to screen cell–particle interactions. A non-thiolated gel 3-D culture matrix (e.g., alginate, PEG, CMC) could

accommodate this requirement in this case, although other cases should be evaluated for other possible analogous particle–matrix interactions. Second, the PT culture media contains many soluble serum proteins known to adsorb to gold surfaces, producing a protein corona [47], and often causing particle aggregation and limited diffusion. Aggregation could also result from divalent cation (e.g., calcium) induced gold particle and gold-HA gel aggregation as well. One approach for overcoming this matrix-binding limitation is to surface-modify gold nanoparticles to reduce interactions with both the HA thiols and serum proteins [48].

Generally, despite controversy with cell culture-based toxicity and gold nanoparticle dosimetry issues *in vitro*, little gold NP toxicity is reported *in vivo* to date in various models, despite widespread biodistribution [14]. Consistent with *in vivo* observations, no gold particle toxicity markers were observed *in vitro*. Nonetheless, the observed heterogeneous gold particle distribution and highly variable local dosing within the HA culture matrix precluded their further utility in this test bed. Therefore, other nanoparticles of interest will require additional modification for use in this culture system, given some issues with transport mechanisms and possible adverse accumulation seen with the gold nanoparticles. It is important to appreciate that problems encountered with HA matrices would be shared with other 3-D matrices that have a charge distribution. This includes many natural polymers and a significant number of synthetic biomaterials.

Nanoparticles as drug carriers and new drug formulations offer several exciting improvements over traditional drug delivery methods, including increased drug bioavailability, extensive range of dosage forms, high carrier capacity and feasibility of incorporating active substances with various physiochemical characteristics [29]. However, before they can be widely implemented with reliable toxicity data accepted by regulatory and environmental monitoring agencies for possible human exposure assessments, several issues associated with particle biocompatibility and assessment tools must be validated. Specifically, nanoparticle toxicity assessment *in vitro* and its predictive relevance and reliability to predicting toxicity *in vivo* are subjects of extensive review, deliberation and investigation [49]. A growing body of literature questions the value and importance of traditional 2-D *in vitro* cell damage/stress assessment assays in cell culture-based screening and toxicity evaluations [5,7–9,25,26,49]. In addition to these concerns, assessment of nano-sized drugs and particles brings an added level of complexity due to both their fundamentally distinct solution properties and technical issues in toxicity testing with cells [15,29]. While many questions about the relationships of surface area, composition (surface chemistry), shape of nanomaterials, and relevant dosimetry on their cell and tissue interactions remaining unanswered, it is difficult to draw conclusions about nano-specific effects in *in vivo* toxicity. Moreover, use of nanoparticles with common commercially available cell viability/proliferation assay kits used for soluble drugs indicates that many can produce misleading information due to particle adsorption and chemical reactions with kit components [50,51].

Gold nanoparticles are a classic case in this regard, with many reported conflicting results. Specifically, cell cultures dosed with nano-gold have exhibited contrasting effects in different cell lines, such as the case of 13 nm nanoparticles tested against human lung and human liver carcinoma cell lines [52]. Similarly, other discrepancies are evident in size-toxicity results. For example, one study suggested that 1.5 nm gold particles *in vivo* could cause liver and spleen damage [22], while another found that 3–5 nm gold nanospheres did not affect lifespan or behavior of BALB/C mice unlike 8–37 nm gold particles [53]. Moreover, many gold particles of different size ranges failed to exhibit toxicity in immortalized cell line cultures. Specifically, 5 nm gold nanoparticles were shown non-toxic to primary HUVEC cells [19] and surfactant-stabilized gold nanorods (65 × 15 nm) showed little observable damage to immortalized human colon carcinoma HT-29 cell line cultures [54]. Controlled particle dosimetry in these cell culture systems is indeed very difficult to control or monitor as shown in comparing 2-D inverted cell cultures for different gold nanoparticle dosings [55].

One 3-D cell culture study [56] described cell toxicity differences for cationic CTAB- and anionic citrate-capped gold nanoparticles of different size and shape dosed to hepatic cell 3-D acrylamide gel culture matrices. Given the distinct surfactant stabilizers bound to each gold nanoparticle preparation, this observed toxicity difference could be attributed to differential intrinsic CTAB versus citrate cell toxicity, including molecular transport/unhindered diffusion of particle-dissociated CTAB vs. citrate through the culture matrix and resulting differences in cell exposure. As neither monitoring of actual gold nanoparticle transport and distribution within these 3-D gels, or gold-surfactant ligand exchange stability was reported following dosing to these cultures, these plausible effects cannot be excluded. Against the backdrop of these highlighted challenges and inconsistencies reported for nano-gold exposures in the literature, there is not much description of nanoparticle dosing/distribution issues within increasingly popular cell-based 3-D culture systems. Given recognized dosimetry issues for particles in 2-D cultures [55], the analogous 3-D culture particle dosing/distribution/transport problem should also be appreciated and countenanced before assessing pharm–tox parameters.

G5-OH PAMAM dendrimers are more readily and reliably assessed using the 3-D PT culture model since their transport was observed to be unhindered in the HA gel matrix. In previous rodent studies, G5-OH injections exhibited almost 80% kidney accumulation in mice when delivered intravenously after only 30 min [23,24]. However, this specific accumulation in kidneys did not increase BUN or creatinine production, two most commonly used clinical assessments of kidney damage [57,58]. Hence, these experiments were corroborated using the 3-D organoid kidney model with accompanying assessments of cellular viability, and multiple common inflammatory cytokine inductions, and kidney cell surface protein biomarker up-regulation. Specifically, proximal tubule death *in vitro* was assessed using dose–response curves and shedding of intracellular NAG enzymes. Both approaches suggested limited cell injury *in vitro* when exposed to doses previously applied *in vivo*. Similarly, PAMAM dendrimers up-regulated one of the most sensitive biomarkers of kidney toxicity, Kim-1, but not TNFα, a biomarker reflecting more acute tissue damage [40,41].

These data collected on tissue injury and surface biomarkers consistently and closely traced changes associated with release of soluble cytokines associated with 3-D cell culture. Specifically, induction of IL-6 typically associated with initiation of drug-induced cellular damage [41,44] was similar to untreated cells and statistically higher than the positive control treatments with cisplatin [41]. Similarly, later steps of the cascade, such as up-regulation of TNFα and/or IL1β, produced identical consistent patterns [41,44]. Other cytokines commonly associated with kidney damage, such as MCP-1, MIP-2, MIP-1β, INFγ and RANTES, exhibited no significant changes in any samples or did not differ from negative controls [41]. The only cytokines statistically significantly up-regulated after exposure to G5-OH dendrimer were IL-2, MIP-1α and anti-inflammatory cytokine, IL-10. These soluble cytokines have general functions of induction of the host immune response via interaction with T cells [59], recruitment of macrophages [60] and promotion of tissue healing [61]. Overall, the data collected from this 3-D PT culture closely reflect those for BUN and creatinine G5-OH exposure data obtained from rodent *in vivo* studies.

Experiments using G5-OH *in vivo* “priming”, that is dendrimer intravenous pre-administration, biodistribution and clearance in a

murine model, followed by isolation of these G5-OH pre-treated kidney PTs for 3-D HA gel 21-day culture, provided contrasting conditions to the direct addition of G5-OH dendrimers to naïve murine-derived PT 3-D cultures for 48 h. Organoid PT cultures from G5-OH pre-exposed kidneys exhibited long-term viability comparable to those from the vehicle-only negative controls (see Fig. 5), supporting the previous studies for G5-OH non-toxicity *in vivo* with these dosing conditions [21,22]. The agreement of *in vitro* extended 3-D PT culture data with this and several other *in vivo* studies for the same nanoparticle dosing is unprecedented and serves as important hallmark for possible predictive success for certain nanoparticle assessments in these systems.

6. Conclusions

We describe extension of previous findings for a 3-D kidney PT organoid model capable of accurately reflecting drug-induced toxicity biomarkers *in vitro* to assess nephrotoxicity markers for nano-sized materials. Potential nanomaterial interactions with the 3-D encapsulation culture matrix and resulting influences on mass transport, dosing and particle distribution within the culture must be thoughtfully considered. Gold nanoparticles were deemed unsuitable for use in these culture: they bound the cell culture polymer hydrogel (HA) matrix and did not transport or distribute. In contrast to gold nanoparticle dosings, dendrimer exposure in these PT 3-D culture models produces a comprehensive set of toxicity indicators, including cytokines, Kim-1 protein induction, cell viability, NAG shedding and cell survival curves that accurately reflect injury data obtained for these dendrimer nanomaterials *in vivo*. These results support the applicability of these 3-D organoid models for kidney toxicity assessments of soluble small molecule and certain nanomaterial agents that can rapidly and reliably distribute to the cultured cells. More significantly, results suggest that the model can provide highly predictive *in vivo–in vitro* comparisons based on extrapolations of *in vivo* dosing regimens. Consistent agreement of dendrimer *in vitro* extended 3-D PT culture responses with dendrimer pre-primed *in vivo* PT-exposed 3-D cultures, and also several other *in vivo* studies is an important validation to prompt other predictive analyses for certain nanoparticle assessments in analogous test beds. Extension of the 3-D culture system to both murine mutant and knock-out models of toxicity as well as to human PTs sourced from cadavers or surgically disposed organs could help validate human predictive toxicity.

Acknowledgements

We thank Dr. J.V. Bonventre (Brigham and Women's Hospital/Harvard Medical School, USA) for generous donation of the R9 Kim-1 antibody and Dr. R. Hitchcock (University of Utah, USA) for contribution of secondary Alexa-488 antibodies. P. Hogrebe is thanked for assistance with illustrations and Dr. C. Rodesch (University of Utah Imaging Facility, USA) for 3-D microscopy imaging. Partial financial support for this work was provided by an Interdisciplinary Seed Grant from the University of Utah, Microgrant from the University of Utah, NIH grants R01DE019050 and R01EB07470, the American Heart Foundation (11POST7290019), and the Utah Science Technology and Research (USTAR) initiative.

Appendix A. Supplementary data

Supplementary data related to this article can be found at http://dx.doi.org/10.1016/j.biomaterials.2014.04.060.

References

[1] Clarke S, Tamang S, Reiss P, Dahan M. A simple and general route for monofunctionalization of fluorescent and magnetic nanoparticles using peptides. Nanotechnology 2011;22(17):175103.
[2] Nel A, Xia T, Madler L, Li N. Toxic potential of materials at the nanolevel. Science 2006;311(5761):622–7.
[3] U.S. demand for nanotechnology medical products to approach $53 Billion in 2011. Meridian Institute; 2007 [cited 2011 12/2/2011]; Available from: http://www.merid.org/Content/News_Services/Nanotechnology_and_Development_News/Articles/2007/05/10/US_Demand_for_Nanotechnology_Medical_Products_to_Approach_53_Billion_in_2011.aspx.
[4] Yoo JW, Irvine DJ, Discher DE, Mitragotri S. Bio-inspired, bioengineered and biomimetic drug delivery carriers. Nat Rev Drug Discov 2011;10(7):521–35.
[5] Hillegass JM, Shukla A, Lathrop SA, MacPherson MB, Fukagawa NK, Mossman BT. Assessing nanotoxicity in cells in vitro. Wiley Interdiscip Rev Nanomed Nanobiotechnol 2010;2(3):219–31.
[6] Balbus JM, Maynard AD, Colvin VL, Castranova V, Daston GP, Denison RA, et al. Meeting report: hazard assessment for nanoparticles–report from an interdisciplinary workshop. Environ Health Perspect 2007;115(11):1654–9.
[7] Heath JR, Davis ME, Hood L. Nanomedicine targets cancer. Sci Am 2009;300(2):44–51.
[8] Heath JR, Davis ME. Nanotechnology and cancer. Annu Rev Med 2008;59:251–65.
[9] Jones CF, Grainger DW. In vitro assessments of nanomaterial toxicity. Adv Drug Deliv Rev 2009;61(6):438–56.
[10] Lewinski N, Colvin V, Drezek R. Cytotoxicity of nanoparticles. Small 2008;4(1):26–49.
[11] Chuang SM, Lee YH, Liang RY, Roam GD, Zeng ZM, Tu HF, et al. Extensive evaluations of the cytotoxic effects of gold nanoparticles. Biochim Biophys Acta 2013;1830(10):4960–73. Epub 2013/07/03.
[12] Astashkina A, Grainger DW. Critical analysis of 3-D organoid in vitro cell culture models for high-throughput drug candidate toxicity assessments. Adv Drug Deliv Rev; 2014. http://dx.doi.org/10.1016/j.addr.2014.02.008.
[13] Lohr JW, Willsky GR, Acara MA. Renal drug metabolism. Pharmacol Rev 1998;50(1):107–42.
[14] Johnston HJ, Hutchison G, Christensen FM, Peters S, Hankin S, Stone V. A review of the in vivo and in vitro toxicity of silver and gold particulates: particle attributes and biological mechanisms responsible for the observed toxicity. Crit Rev Toxicol 2010;40(4):328–46.
[15] Fadeel B, Garcia-Bennett AE. Better safe than sorry: understanding the toxicological properties of inorganic nanoparticles manufactured for biomedical applications. Adv Drug Deliv Rev 2010;62(3):362–74.
[16] Goodman CM, McCusker CD, Yilmaz T, Rotello VM. Toxicity of gold nanoparticles functionalized with cationic and anionic side chains. Bioconjug Chem 2004;15(4):897–900.
[17] Jahnen-Dechent W, Simon U. Function follows form: shape complementarity and nanoparticle toxicity. Nanomedicine (Lond) 2008;3(5):601–3.
[18] Lundqvist M, Stigler J, Elia G, Lynch I, Cedervall T, Dawson KA. Nanoparticle size and surface properties determine the protein corona with possible implications for biological impacts. Proc Natl Acad Sci U S A 2008;105(38):14265–70.
[19] Esther RJ, Bhattacharya R, Ruan M, Bolander ME, Mukhopadhyay D, Sarkar G, et al. Gold nanoparticles do not affect the Global Transcriptional Program of human umbilical vein endothelial cells: a DNA-microarray analysis. J Biomed Nanotechnol 2005;1(3):328–35.
[20] Tsai CY, Shiau AL, Chen SY, Chen YH, Cheng PC, Chang MY, et al. Amelioration of collagen-induced arthritis in rats by nanogold. Arthritis Rheum 2007;56(2):544–54.
[21] Mukherjee P, Bhattacharya R, Wang P, Wang L, Basu S, Nagy JA, et al. Antiangiogenic properties of gold nanoparticles. Clin Cancer Res 2005;11(9):3530–4.
[22] Khlebtsov N, Dykman L. Biodistribution and toxicity of engineered gold nanoparticles: a review of in vitro and in vivo studies. Chem Soc Rev 2011;40(3):1647–71.
[23] Sadekar S, Ghandehari H. Transepithelial transport and toxicity of PAMAM dendrimers: implications for oral drug delivery. Adv Drug Deliv Rev 2012;64(6):571–88.
[24] Sadekar S, Ray A, Janat-Amsbury M, Peterson CM, Ghandehari H. Comparative biodistribution of PAMAM dendrimers and HPMA copolymers in ovarian-tumor-bearing mice. Biomacromolecules 2011;12(1):88–96.
[25] Astashkina AI, Mann BK, Prestwich GD, Grainger DW. Comparing predictive drug nephrotoxicity biomarkers in kidney 3-D primary organoid culture and immortalized cell lines. Biomaterials 2012;33(18):4712–21.
[26] Astashkina AI, Mann BK, Prestwich GD, Grainger DW. A 3-D organoid kidney culture model engineered for high-throughput nephrotoxicity assays. Biomaterials 2012;33(18):4700–11.
[27] Chen J, Dongre A. Improving the pharmaceutical properties of biologics in drug discovery: unique challenges and enabling solutions. ADME – Enabling Technologies in Drug Design and Development. John Wiley & Sons, Inc; 2012. pp. 67–77.
[28] Longmire M, Choyke PL, Kobayashi H. Clearance properties of nano-sized particles and molecules as imaging agents: considerations and caveats. Nanomedicine (Lond) 2008;3(5):703–17.

[29] Grainger DW. Nanotoxicity assessment: all small talk? Adv Drug Deliv Rev 2009;61(6):419–21.
[30] Alkilany AM, Murphy CJ. Toxicity and cellular uptake of gold nanoparticles: what we have learned so far? J Nanopart Res 2010;12(7):2313–33.
[31] Godek ML, Michel R, Chamberlain LM, Castner DG, Grainger DW. Adsorbed serum albumin is permissive to macrophage attachment to perfluorocarbon polymer surfaces in culture. J Biomed Mater Res 2009;88(2):503–19.
[32] Schneider G, Decher G. Functional core/shell nanoparticles via layer-by-layer assembly. Investigation of the experimental parameters for controlling particle aggregation and for enhancing dispersion stability. Langmuir 2008;24(5):1778–89.
[33] Frens G. Controlled nucleation for the regulation of the particle size in monodisperse gold suspensions. Nat Phys Sci 1973;241:20–2.
[34] Kitchens KM, Kolhatkar RB, Swaan PW, Eddington ND, Ghandehari H. Transport of poly(amidoamine) dendrimers across Caco-2 cell monolayers: influence of size, charge and fluorescent labeling. Pharm Res 2006;23(12):2818–26.
[35] Jones CF, Campbell RA, Franks Z, Gibson CC, Thiagarajan G, Vieira-de-Abreu A, et al. Cationic PAMAM dendrimers disrupt key platelet functions. Mol Pharmacol 2012;9(6):1599–611. Epub 2012/04/14.
[36] Lasagna-Reeves C, Gonzalez-Romero D, Barria MA, Olmedo I, Clos A, Sadagopa Ramanujam VM, et al. Bioaccumulation and toxicity of gold nanoparticles after repeated administration in mice. Biochem Biophys Res Commun 2010;393(4):649–55.
[37] Nishimura K, Kawada M, Suehiro T, Yamano T, Hashimoto K. Urinary N-acetyl-beta-D-glucosaminidase and gamma-glutamyl-transpeptidase activities for evaluation of renal disturbance in patients with multiple myeloma. Nihon Jinzo Gakkai Shi 1992;34(10):1087–94.
[38] Barcelos LS, Talvani A, Teixeira AS, Vieira LQ, Cassali GD, Andrade SP, et al. Impaired inflammatory angiogenesis, but not leukocyte influx, in mice lacking TNFR1. J Leukoc Biol 2005;78(2):352–8.
[39] Sadekar S, Ghandehari H. Transepithelial transport and toxicity of PAMAM dendrimers: implications for oral drug delivery. Adv Drug Deliv Rev 2012;64(6):571–88.
[40] Huo W, Zhang K, Nie Z, Li Q, Jin F. Kidney injury molecule-1 (KIM-1): a novel kidney-specific injury molecule playing potential double-edged functions in kidney injury. Transpl Rev Orl 2010;24(3):143–6.
[41] Akcay A, Nguyen Q, Edelstein CL. Mediators of inflammation in acute kidney injury. Mediators Inflamm 2009;2009:137072.
[42] Davis JW, Kramer JA. Genomic-based biomarkers of drug-induced nephrotoxicity. Expert Opin Drug Metab Toxicol 2006;2(1):95–101.
[43] Sieber M, Hoffmann D, Adler M, Vaidya VS, Clement M, Bonventre JV, et al. Comparative analysis of novel noninvasive renal biomarkers and metabonomic changes in a rat model of gentamicin nephrotoxicity. Toxicol Sci 2009;109(2):336–49.
[44] Ramesh G, Reeves WB. TNF-alpha mediates chemokine and cytokine expression and renal injury in cisplatin nephrotoxicity. J Clin Invest 2002;110(6):835–42.
[45] Prestwich GD. Evaluating drug efficacy and toxicology in three dimensions: using synthetic extracellular matrices in drug discovery. Acc Chem Res 2008;41(1):139–48.
[46] Prestwich GD. Hyaluronic acid-based clinical biomaterials derived for cell and molecule delivery in regenerative medicine. J Control Release 2011;155(2):193–9.
[47] Zhang D, Neumann O, Wang H, Yuwono VM, Barhoumi A, Perham M, et al. Gold nanoparticles can induce the formation of protein-based aggregates at physiological pH. Nano Lett 2009;9(2):666–71.
[48] Bomke S, Sperling M, Karst U. Organometallic derivatizing agents in bioanalysis. Anal Bioanal Chem 2010;397(8):3483–94.
[49] Astashkina A, Mann B, Grainger DW. A critical evaluation of in vitro cell culture models for high-throughput drug screening and toxicity. Pharmacol Ther 2012;134(1):82–106.
[50] Alkilany AM, Frey RL, Ferry JL, Murphy CJ. Gold nanorods as nanoadmicelles: 1-naphthol partitioning into a nanorod-bound surfactant bilayer. Langmuir 2008;24(18):10235–9.
[51] Willets KA, Van Duyne RP. Localized surface plasmon resonance spectroscopy and sensing. Annu Rev Phys Chem 2007;58:267–97.
[52] Patra HK, Banerjee S, Chaudhuri U, Lahiri P, Dasgupta AK. Cell selective response to gold nanoparticles. Nanomedicine 2007;3(2):111–9.
[53] Chen YS, Hung YC, Liau I, Huang GS. Assessment of the in vivo toxicity of gold nanoparticles. Nanoscale Res Lett 2009;4(8):858–64.
[54] Alkilany AM, Nagaria PK, Hexel CR, Shaw TJ, Murphy CJ, Wyatt MD. Cellular uptake and cytotoxicity of gold nanorods: molecular origin of cytotoxicity and surface effects. Small 2009;5(6):701–8.
[55] Cho EC, Zhang Q, Xia Y. The effect of sedimentation and diffusion on cellular uptake of gold nanoparticles. Nat Nanotechnol 2011;6(6):385–91. Epub 2011/04/26.
[56] Lee J, Lilly GD, Doty RC, Podsiadlo P, Kotov NA. In vitro toxicity testing of nanoparticles in 3D cell culture. Small 2009;5(10):1213–21.
[57] Tseng SC, Lee PC, Ells PF, Bissell DM, Smuckler EA, Stern R. Collagen production by rat hepatocytes and sinusoidal cells in primary monolayer culture. Hepatology 1982;2(1):13–8.
[58] Davis 2nd JW, Goodsaid FM, Bral CM, Obert LA, Mandakas G, Garner 2nd CE, et al. Quantitative gene expression analysis in a nonhuman primate model of antibiotic-induced nephrotoxicity. Toxicol Appl Pharmacol 2004;200(1):16–26.
[59] Savransky V, Molls RR, Burne-Taney M, Chien CC, Racusen L, Rabb H. Role of the T-cell receptor in kidney ischemia-reperfusion injury. Kidney Int 2006;69(2):233–8.
[60] Keepers TR, Gross LK, Obrig TG. Monocyte chemoattractant protein 1, macrophage inflammatory protein 1 alpha, and RANTES recruit macrophages to the kidney in a mouse model of hemolytic-uremic syndrome. Infect Immun 2007;75(3):1229–36.
[61] Kim MG, Yang HN, Kim HW, Jo SK, Cho WY, Kim HK. IL-10 mediates rosiglitazone-induced kidney protection in cisplatin nephrotoxicity. J Korean Med Sci 2010;25(4):557–63.